On recirculating flow in an opposed jet flame holder

S. Majumdar and D. Bhaduri

Central Mechanical Engineering Research Institute, Durgapur-713209, India
(Received July 1980)

Introduction

The analysis of ducted jets with recirculation has received much attention in recent years[1–4] because of its potential application in high speed combustion systems to obtain enhanced mixing and stable flame. In an opposed-jet flame stabilization system, a small jet of high velocity gas flows in a direction opposite to the confined mainstream of pre-mixed combustible mixture. The stagnation zone created by the interaction of the jet and the mainstream provides the required locally decelerated region and the recirculation of the hot products of combustion is effected due to the jet entrainment in the confined mainstream.

Since its inception as a potential flame holder,[1] experimental work[1–7] has been reported on the opposed-jet system which reveal some gross-behaviour of the flow pattern, but theoretical research on such a flow system for predicting the flow parameters is, however, meagre. A complete analysis of the flow-field demands the simultaneous solution of the relevant differential equations governing the conservation of mass, momentum and energy using the appropriate mathematical model for the different physical and chemical processes involved. The simple 'integral methods' proposed by a group of Soviet research workers[5–7] for the prediction of the flow field for isothermal and also the reacting situation for the opposed-jet system are seriously limited by the boundary layer assumptions which are not strictly valid in recirculating flows. It is only recently that a general numerical method has been available for solving the elliptic partial differential equations for turbulent, recirculating flows.

Here, a simplified mathematical model of the flow of a non-reacting turbulent jet spreading into a ducted, uniform, counterflowing stream is proposed. The numerical method of Gosman *et al.*[8] is applied to predict the flow parameters in the isothermal situation of an opposed-jet flame holder. Experimental investigations are also carried out for comparison of experimental results with the prediction to validate the prediction procedure.

Mathematical modelling

Governing equations

With reference to the axisymmetric two-dimensional co-ordinate system shown in *Figure 1*, the governing differential equations for stream-function and vorticity are given below:

Stream function:

$$\frac{\partial}{\partial x}\left(\frac{1}{\rho r}\frac{\partial \psi}{\partial x}\right)+\frac{\partial}{\partial r}\left(\frac{1}{\rho r}\frac{\partial \psi}{\partial r}\right)+\omega=0 \qquad (1)$$

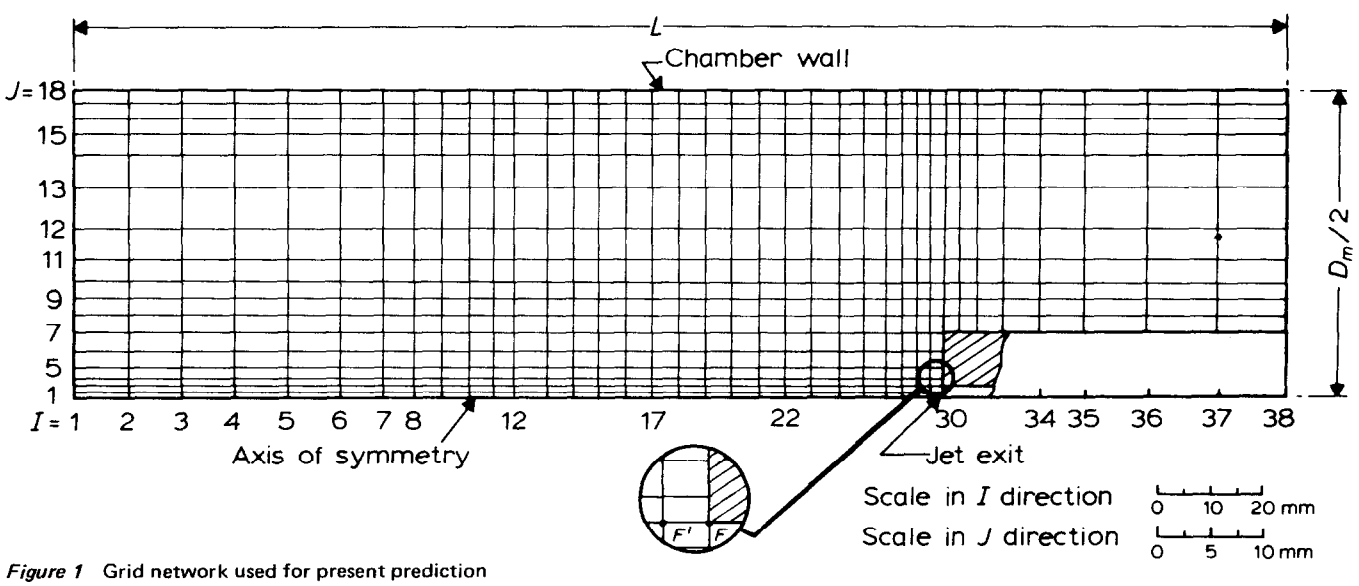

Figure 1 Grid network used for present prediction

0307-904X/81/030179-06/$02.00

Vorticity:

$$r^2\left[\frac{\partial}{\partial x}\left(\frac{\omega}{r}\frac{\partial\psi}{\partial r}\right)-\frac{\partial}{\partial r}\left(\frac{\omega}{r}\frac{\partial\psi}{\partial x}\right)\right]-\frac{\partial}{\partial x}\left[r^3\frac{\partial}{\partial x}\left(\mu_{\text{eff}}\frac{\omega}{r}\right)\right]-\frac{\partial}{\partial r}\left[r^3\frac{\partial}{\partial r}\left(\mu_{\text{eff}}\frac{\omega}{r}\right)\right]=0 \quad (2)$$

where the stream-function, ψ, satisfies the continuity equation and is defined as:

$$u=\frac{1}{\rho r}\frac{\partial\psi}{\partial r} \quad (3)$$

$$v=-\frac{1}{\rho r}\frac{\partial\psi}{\partial x} \quad (4)$$

$$\omega=\frac{\partial v}{\partial x}-\frac{\partial u}{\partial r} \quad (5)$$

Equations (1) and (2) are solved simultaneously for the prediction of the distribution of stream-function, vorticity; consequently the velocity field is available from equations (3) and (4).

Turbulence modelling

The effect of turbulence in equation (2) is taken into account using an effective transport coefficient, μ_{eff}, which may vary from point to point throughout the field and is to be calculated according to any of the available mathematical models of turbulence.[9] In the present work, a simple *ad hoc* formula proposed by Pun and Spalding[10] has been used for the effective viscosity:

$$\mu_{\text{eff}}=KD_m^{2/3}L^{-1/3}\rho^{2/3}\left[W_mV_m^2+W_jV_j^2\right]^{1/3} \quad (6)$$

where, D_m and L are dimensions shown in *Figure 1*. The term $[W_mV_m^2+W_jV_j^2]$ is the mean kinetic energy of the fluid entering the system and ρ is the local density of the mixture. A value of 0.012 has been used for the constant K as suggested by the successful prediction of recirculating flow situations.[10–13]

Boundary conditions

In view of the symmetry of the flow-field about the central axis, the domain of integration has been limited to half the cross-section of the main duct.

Inlet

The flow at both main and jet stream inlets are assumed to be of uniform velocity. Therefore, the stream function and the vorticity at inlets are given by:

$$\text{Main inlet: } \frac{\omega}{r}=0 \qquad \psi(r)=0.5\rho V_m r^2 \quad (7)$$

$$\text{Jet inlet: } \frac{\omega}{r}=0 \qquad \psi(r)=0.5\rho V_j r^2 \quad (8)$$

Exit

At the exit section, the longitudinal gradients of vorticity and stream function have been assumed to vanish:

$$\frac{\partial}{\partial x}(\omega/r)=0 \quad (9)$$

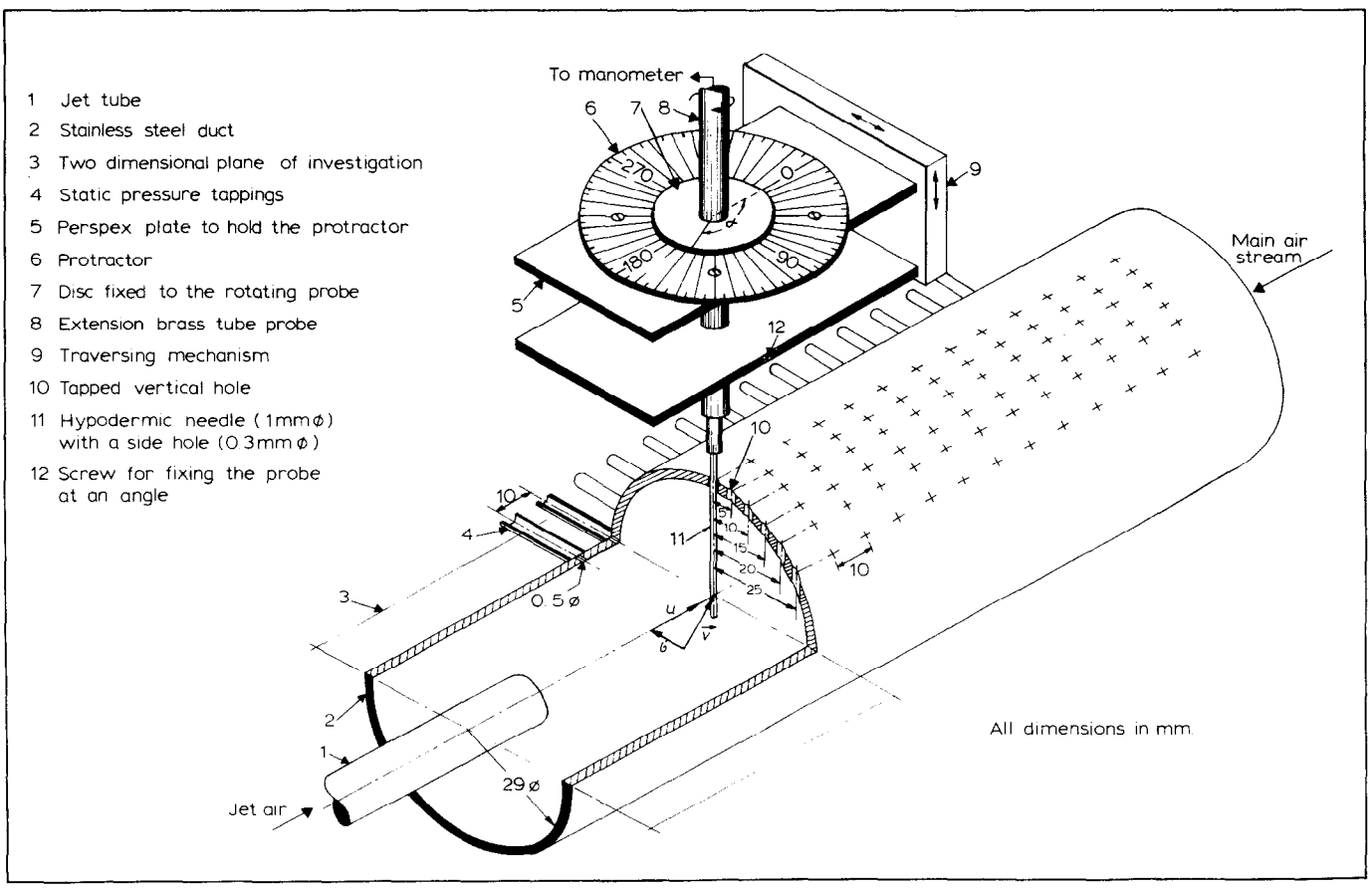

Figure 2 Test section for isothermal study showing cross-section of an axial station

$$\frac{\partial \psi}{\partial x} = 0 \qquad (10)$$

Axis of symmetry

Along the axis of symmetry, the stream function and the vorticity are both assumed to be zero. But the dependent variable ω/r representing the vorticity in axisymmetric situations is finite in magnitude at $r = 0$. ω/r at the axis is evaluated using a quadratic approximation for the vorticity profile between the axis of symmetry and the two other adjacent nodes near the axis along the radial direction.

Walls

Along a solid wall, the stream function is constant. The magnitude of the constants are determined by the flow rate of fluid through the inlet ports. The expression for vorticity contains velocity gradients and is difficult to specify in advance. The computation of vorticity has been made on the assumption that a Couette flow layer exists near the solid walls where the longitudinal convection terms may be neglected. For the different vertical and horizontal walls in the field, the wall vorticities are always linked to the vorticity at a near wall node and an implicit formulation[10] has been used to include the effect of wall vorticities in calculating the field for the stream-function and vorticity.

Protruding corners

The evaluation of vorticity at a protruding corner (F in *Figure 1*) according to the general treatment of the near wall region is difficult because the assumption of a Couette flow parallel to the wall is not obvious for a corner. The vorticity at the corner node is therefore computed by a special method suggested by Pun and Spalding.[10] The stream functions at F and F' (*Figure 1*) are assumed to be equal from physical considerations. Then the vorticity at the near corner node (F') is evaluated from the finite-difference equation for the stream function at the same node where the vorticity also appears as a source term.

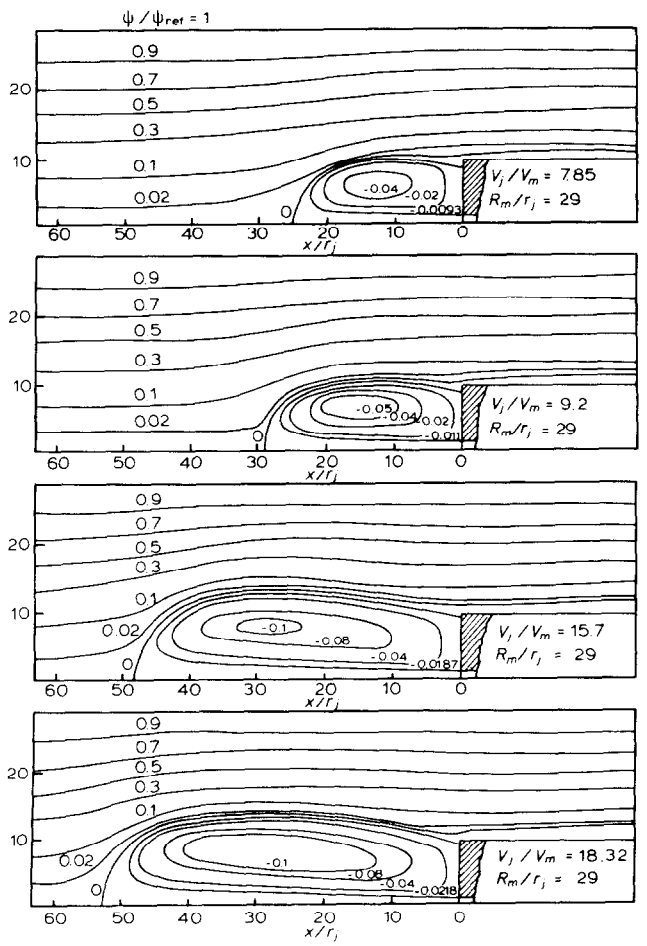

Figure 3 Effect of velocity ratio (V_j/V_m) on flow pattern

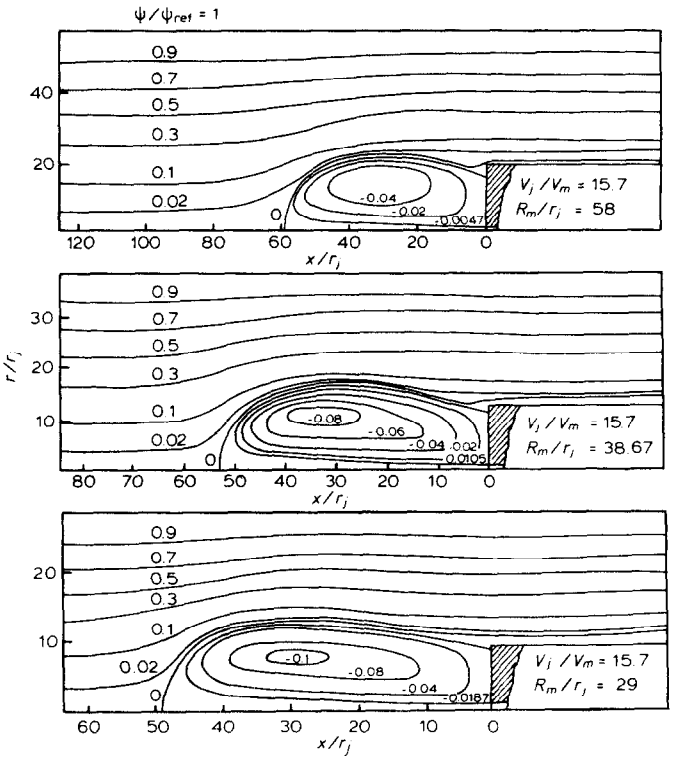

Figure 4 Effect of radius ratio (R_m/r_j) on flow pattern

Computational details

The geometry of the present numerical prediction is shown in *Figure 1*. 38 (x-direction) x 18 (r-direction) non-uniform grids are used for predicting different experimental situations. Only very large radius ratios (R_m/r_j) necessitated the use of 20 radial grid lines. The uniform flow velocity at the jet inlet which is required as a physical input to the prediction procedure is evaluated from the measured upstream pressure and temperature of the jet fluid. The details of this measurement and calculation are given elsewhere.[14]

Experiment

The measurement of velocity profiles has been carried out in a stainless steel duct of internal diameter 58 mm. A concentric jet assembly of outside diameter 12 mm is introduced from the open end of the test section. A special arrangement is provided to fix nozzles of different sizes to the end of the jet assembly. *Figure 2* shows the test section and the arrangement for measuring the axisymmetric two-dimensional velocity field. A calibrated single hole cylindrical probe, as shown in *Figure 2*, is used for sensing the magnitude and direction of the total head. The static pressure at any longitudinal section is sensed from the wall tappings at the respective sections. A two-dimensional traversing arrangement is used for scanning the flow-field

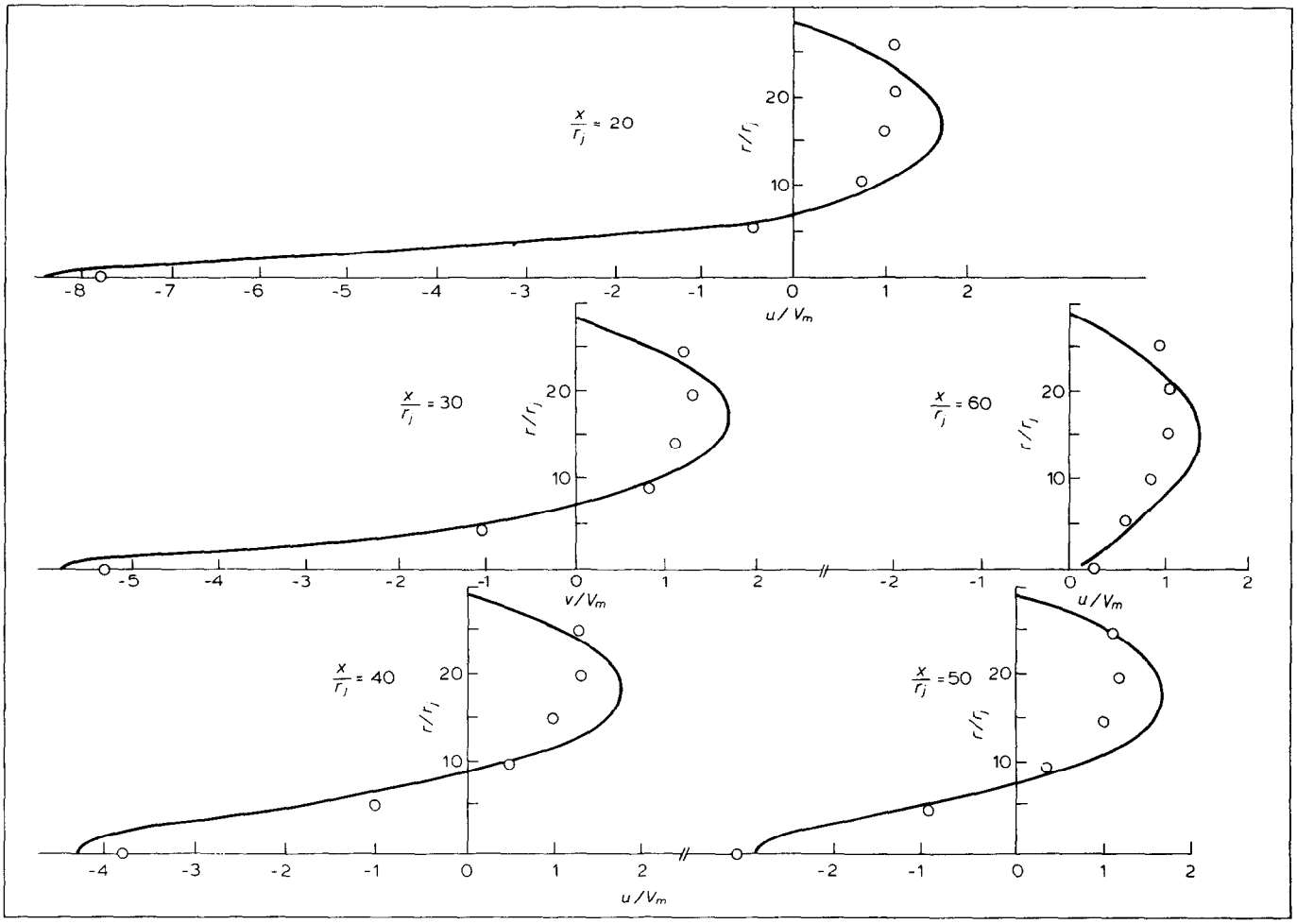

Figure 5 Distribution of longitudinal velocity. $V_j/V_m = 17.8$; $R_m/r_j = 29$. (o), measurement; (—), prediction by numerical method

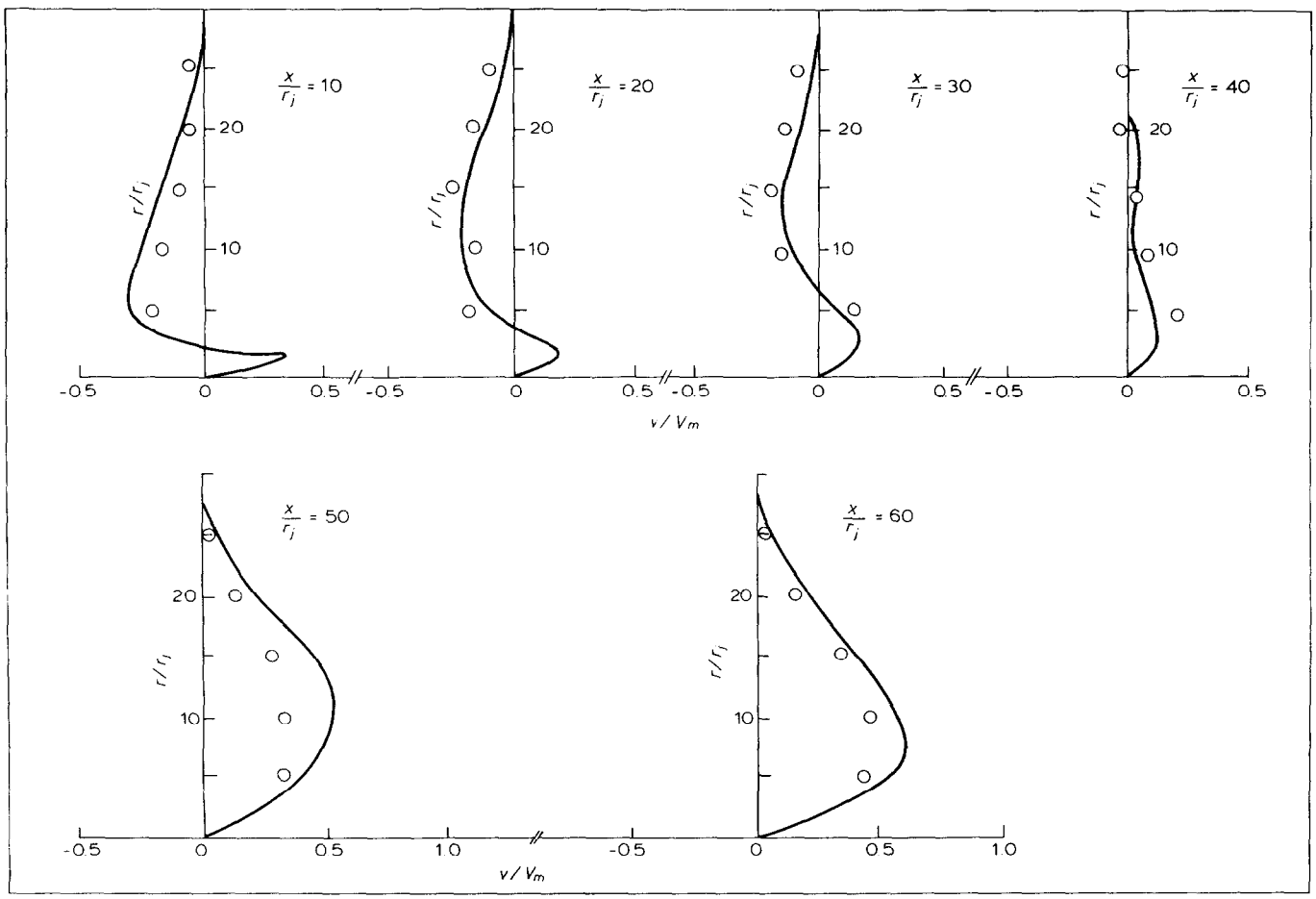

Figure 6 Distribution of transverse velocity. (Key as in *Figure 5*.)

at the desired points. The details of the experimental set up and measurement techniques have been described elsewhere.[14]

Results and discussion

The normalized stream-function distributions obtained from parametric computation employing the present prediction procedure are presented in *Figures 3* and *4*, which show the effects of the velocity ratio (V_j/V_m) and radius ratio (R_m/r_j) on the flow pattern. The figures clearly display the formation of a recirculation region and also a stagnation surface ($\psi = 0$), originating from a stagnation point on the axis separating the mainstream and the recirculating flow regions. The observed shift of the stagnation point further upstream away from the jet mouth and the increase in the size of the recirculation zone with an increase of velocity ratio or decrease of radius ratio may be explained physically by the increased momentum of the jet fluid relative to that of the mainstream.

Figures 5 and *6* show a comparison between the experimental results and the numerical predictions of the longitudinal and transverse velocities for a particular velocity ratio and radius ratio. The observed discrepancies, especially in the region outside the reverse flow zone may be attributed to the approximation in the turbulence modelling. The use of a constant effective viscosity over the whole field in conjunction with the wall flux relationship[10] for vorticity seems to have overpredicted the wall shear leading to a velocity profile much steeper than that observed in experiments.

The decay of the jet velocity along the axis of symmetry is shown in a normalized form in *Figure 7* for different velocity ratios. The experimental results are observed to compare reasonably well with the prediction. *Figure 8* also shows a satisfactory agreement between the prediction and the experimental results for the relative jet penetration length (L_p/r_j).

The maximum reverse mass flow rate, which is a measure of the strength of recirculation has been calculated from the predicted velocity distribution and is shown in *Figure 9* for different values of velocity and diameter ratios. It is interesting to note that in an opposed-jet system, an external supply of a very small mass flow (1 to 2% of the main flow) in the reverse direction creates a recirculation zone where the reverse flow intensity (W_{rev}/W_m) is of the order of even 10 to 12% of the mainflow for high velocity ratios.

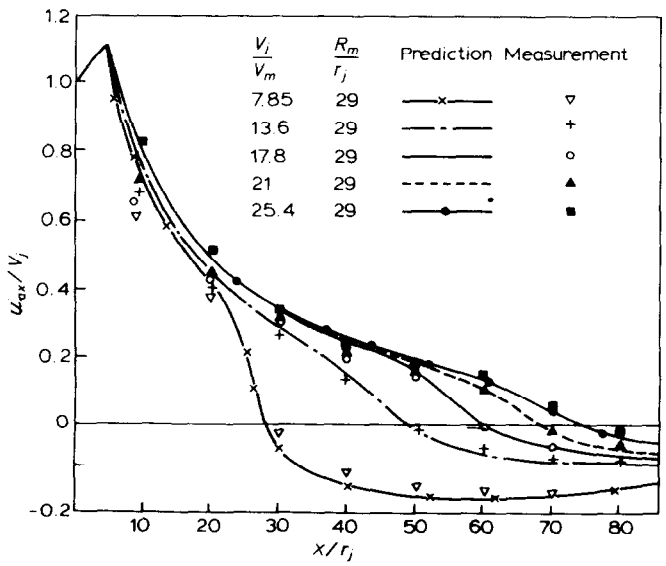

Figure 7 Decay of jet velocity along axis of symmetry

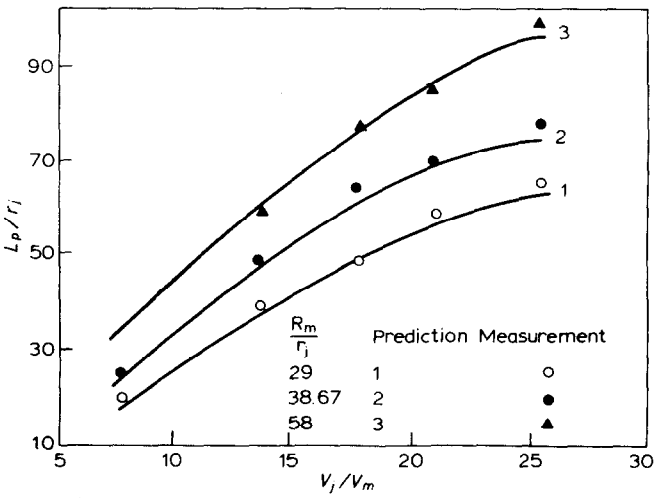

Figure 8 Variation of relative penetration length of jet

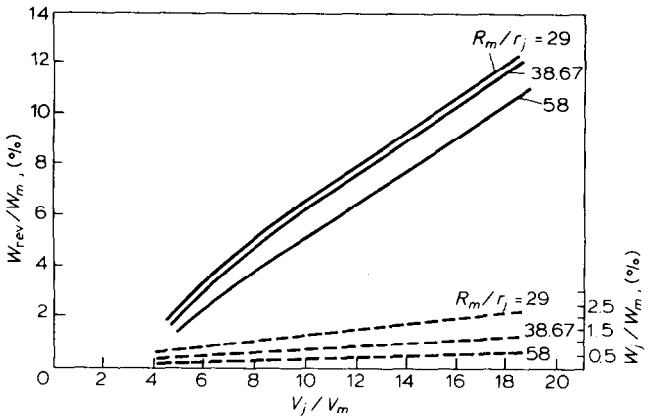

Figure 9 Variation of maximum reverse mass flow rate with velocity ratio for different radius ratios (—), maximum reverse mass flow rate, W_{rev}/W_m (– – –), supplied jet mass flow rate W_j/W_m

Conclusions

The comparison between experimental results and the present predictions shows that the flow of a turbulent jet in a counterflowing, concentric, ducted uniform stream is amenable to theoretical analysis by numerical solution of the governing differential equations. The agreement is also sufficient to justify calculation for some of the important features of the flow such as the jet penetration length, the axial velocity decay, etc. However, the discrepancies between the predicted and measured velocity distribution may be attributed mainly to the inadequate turbulence modelling. A more accurate prediction is possible by using higher order models of turbulence.

Acknowledgements

The authors acknowledge the assistance of Dr A. K. Majumdar of CMERI in the numerical solution of the problem. Thanks are due to Mr D. Maji for his co-operation in the experimental work and to Mr B. M. Sen for typing the manuscript. The Director, CMERI, is thanked for permission to publish this work.

References

1 Schaffer, A. B. and Cambel, A. B. *Jet Propulsion*, 1955, **25**, 284
2 Eustis, R. H. and Mraz, C. L. *WADC* TN 56-316, 1956
3 Noreen, A. E. and Martin, W. T. American Rocket Society, Paper 515-57, 1957
4 O'Loughlin, J. R. Report of Tulane University, New Orleans, Louisana, 1968
5 Vulis, L. A. and Leont'yeva, T. A. *Izv. Akad. Kaz., SSR, Ser. Energ.*, no. 9, 1955
6 Sui, Kh. N. *Izv. Est. SSR, Ser. Tekhn, i., Fiz.-Mat. Nauk*, **10**, no. 3, 1961
7 Sekundov, A. N. 'Turbulent jets of air, plasma and real gases' (Ed. Abramovich, G. N.), Consultants Bureau, New York 1969
8 Gosman, A. D. *et al.* 'Heat and mass transfer in recirculating flows', Academic Press, London, 1969
9 Launder, B. E. and Spalding, D. B. 'Mathematical models of turbulence', Academic Press, London, 1972
10 Pun, W. M. and Spalding, D. B. Imperial College, Rep. No. SF/TN/11, 1967
11 Odlozinski, G. Imperial College, Rep. No. EF/R/G/2, 1968
12 Majumdar, A. K. and Bhaduri, D. *Appl. Math. Modelling*, 1976, **1**, 125
13 Kundu, K. M. *et al. Appl. Math. Modelling*, 1977, **1**, 276
14 Majumdar, S. *PhD Thesis*, University of Burdwan, 1979

Nomenclature

D_m	Diameter of main stream
L	Length of chamber
L_p	Jet penetration length measured from jet mouth
R_m	Radius of mainstream
r_j	Radius of jet stream
r	Distance along radial direction
u	Longitudinal velocity
u_{ax}	Longitudinal velocity on axis
v	Transverse velocity
V_j	Velocity of jet stream at inlet
V_m	Velocity of mainstream at inlet
W_j	Mass flow rate of jet stream
W_m	Mass flow rate of main stream
W_{rev}	Maximum reverse mass flow rate
x	Distance along longitudinal direction
μ_{eff}	Effective viscosity
ρ	Density
ψ	Stream function
ω	Vorticity